

Electric-Susceptibility Hole Mass of Lead Telluride

JACK R. DIXON AND H. R. RIEDL

U. S. Naval Ordnance Laboratory, White Oak, Silver Spring, Maryland

(Received 7 December 1964)

Experimental values of the electric-susceptibility hole mass m_s of PbTe are given for temperatures ranging from 24 to 300°K and carrier concentrations from 3.5×10^{18} to 4.8×10^{19} cm $^{-3}$. The masses are deduced from measurements of infrared reflectivity using the method of Spitzer and Fan. The mass increases monotonically with increasing temperature and carrier concentration in a way which indicates strong nonparabolicity of the valence band. The carrier-concentration dependence at 30°K is explained in terms of a single-band, nonparabolic multivalley model and the band-edge parameters reported by Cuff, Ellett, Kuglin, and Williams. The constant-energy surfaces involved are $\langle 111 \rangle$ prolate surfaces of revolution located at the zone boundaries. The temperature dependence of m_s for a carrier concentration of 3.5×10^{18} cm $^{-3}$ can also be explained in terms of this single-band model. The agreement depends upon the assumption that the interaction gap varies linearly with temperature in the same way as the optical gap, the coefficient being 4.9×10^{-4} eV/°K. For a carrier concentration of 4.8×10^{19} cm $^{-3}$, the single-band model does not yield results which are consistent with the observed values of m_s as a function of temperature, except at the lowest temperature of 30°K. Differences between calculation and experiment at higher temperatures suggest that a second band becomes appreciably populated.

I. INTRODUCTION

THERE have been many experimental studies of the valence-band structure of lead telluride during the past few years.¹ These studies have established the existence of $\langle 111 \rangle$ prolate-ellipsoidal energy surfaces at the zone boundaries. The surfaces are believed to be strongly nonparabolic at low temperatures.^{2,3} There is, also, evidence for the existence of other populated bands.⁴⁻⁹ Unfortunately, considerable uncertainty remains concerning the appropriate over-all valence-band model and its parameters. Part of the difficulty is that the experiments which have given direct information about individual band parameters often have been limited to low temperatures and to a relatively small range of carrier concentrations. For this reason, many of the desirable tests of proposed models have not been made. The measurements of the electric-susceptibility hole mass m_s which we are reporting here were made for the purpose of carrying out such tests over large ranges of temperature and carrier concentration. This mass is directly related to the band masses near the Fermi energy. For the case of PbTe, it depends upon the

temperature and carrier concentration in a way which is sensitive to the types of energy surfaces involved. Therefore, such measurements serve as a stringent consistency test of proposed band models and their parameters.

Our experimental method, details of data analysis, and results are described in Secs. II and IV. In Sec. III, the equations which relate m_s to the pertinent types of constant-energy surfaces are reviewed or developed. Finally, in Sec. V, we compare our experimental results with those calculated on the basis of proposed band models and discuss the implications.

II. EXPERIMENTAL

Susceptibility masses were determined from measurements in the infrared region of the frequency dependence of the spectral reflectivity R at normal incidence. The method was first described and applied by Spitzer and

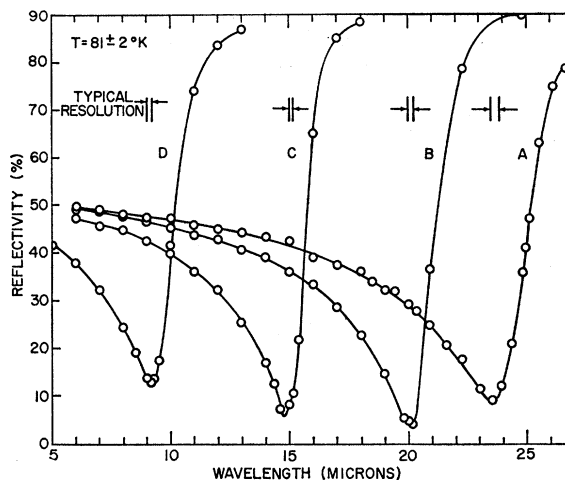


FIG. 1. Wavelength dependence of the normal reflectivity at 81°K for p -type PbTe samples of various carrier concentrations. Electrical properties of these samples are given in Table I.

¹ References through 1958 are given in W. W. Scanlon, *Solid State Phys.* **9**, 83 (1959). A complete listing of more recent publications is not given here but can be easily compiled using the papers which we reference.

² C. F. Cuff, M. R. Ellett, and C. D. Kuglin, *Proceedings of the International Conference on the Physics of Semiconductors, Exeter* (The Institute of Physics and the Physical Society, London, 1962), p. 316.

³ K. F. Cuff, M. R. Ellett, C. D. Kuglin, and L. R. Williams, *Physics of Semiconductors, Proceedings of the 7th International Conference, Paris* (Dunod Cie., Paris, 1964), p. 677.

⁴ R. S. Allgaier, *J. Appl. Phys. Suppl.* **32**, 2185 (1961).

⁵ P. J. Stiles, E. Burstein, and D. N. Langenberg, *J. Appl. Phys. Suppl.* **32**, 2174 (1961).

⁶ R. H. Rediker and A. R. Calawa, *J. Appl. Phys. Suppl.* **32**, 2189 (1961).

⁷ H. R. Riedl, *Phys. Rev.* **127**, 162 (1962).

⁸ J. R. Dixon and H. R. Riedl, *Proceedings of the International Conference on the Physics of Semiconductors, Exeter* (The Institute of Physics and the Physical Society, London, 1962), p. 179.

⁹ R. S. Allgaier and B. B. Houston, Jr. (private communication).

Fan.¹⁰ Our measurements of R were carried out in the exit optics of a Model 99 Perkin-Elmer monochromator. The optical system was designed to provide an angle of incidence of approximately 10 deg. The reflectivity at this angle is expected to differ from that obtained at normal incidence by less than 0.3%. A cesium bromide prism was used throughout the wavelength region from 4 to 30 μ . Typical resolutions are indicated in Fig. 1. Sample temperatures were varied by placing the samples in an optical Dewar similar to the one described by Duerig and Mador.¹¹ Temperatures were measured to within $\pm 1^\circ\text{K}$ using a copper-constantan thermocouple attached to the edge of the sample with silver paste.

Optical samples of p -type PbTe were cut from pulled crystals prepared and supplied by B. B. Houston, Jr.,¹² of our laboratory. Material prepared in this manner normally had a hole concentration of approximately $4 \times 10^{18} \text{ cm}^{-3}$ (sample A). Other carrier concentrations were obtained by heat treatment¹³ (sample B) or by doping the melt with sodium (samples C and D).

The measured reflectivities of these samples were dependent upon the method used to prepare optical surfaces. When mechanical polishing techniques were employed, reflectivities in the wavelength region of the reflectivity minimum depended strongly upon the nature of the polishing process and were not reproducible. Reproducible results were obtained, however, by using an electrolytic polishing technique developed by M. K. Norr.¹⁴ This polish produced a smooth, mirror-like surface. Laue back-reflection x-ray diffraction patterns from electropolished surfaces were well defined, indicating good crystalline structure within a surface layer of thickness corresponding approximately to the x-ray penetration depth. This penetration depth was made small by using a relatively low x-ray tube voltage of 10 kV and long exposure times of over 9 h. An estimate based upon the x-ray short-wavelength cutoff of 1.24 \AA and the mass absorption coefficients of lead and tellurium indicates that the maximum x-ray penetration depth was less than 8μ . The fact that the penetration depth of the infrared light used in the reflectivity measurements was normally greater than 8μ indicates that reflectivities from electrolytically polished surfaces are characteristic of the bulk crystalline material rather than a damaged surface layer.

Carrier concentrations N and conductivity mobilities μ were determined from measurements of the low-field Hall coefficient R_0 and the conductivity σ , using the relations:

$$N = r/|R_0|e,$$

$$\mu = |R_0|\sigma/r.$$

In these expressions, $r = R_\infty/R_0$, where R_∞ is the high-

TABLE I. Electrical properties of p -type PbTe samples at 77.4°K.

Sample	Carrier concentration (cm^{-3})	Conductivity ($\text{cm}^2/\text{V sec}$)	Optical mobility* ($\text{cm}^2/\text{V sec}$)
A	3.5×10^{18}	18 000	7800
B	5.7×10^{18}	15 000	9400
C	1.5×10^{19}	9400	3300
D	4.8×10^{19}	2400	720

* Optical mobilities were determined by fitting reflectivity curves calculated on the basis of classical free-carrier dispersion theory to our experimental data. These data apply to temperatures of $81 \pm 2^\circ\text{K}$.

field Hall coefficient. We have used an r of 0.88 over our entire range of carrier concentrations. This represents an average of the values determined from the magnetic-field dependence of the Hall coefficient reported by Allgaier.⁴ Electrical properties of our optical samples are given in Table I. The mobilities are typical of those reported previously.¹⁵

III. THEORY

A. Classical Treatment of Dispersion Due to Free Carriers

The free-carrier dispersion of the real and imaginary parts of the dielectric constant, ϵ_1 and ϵ_2 , depends upon the electric susceptibility mass of the carriers involved. It gives rise to our experiments to a frequency dependence of the reflectivity R measured at near-normal incidence. The relationship between m_s and the frequency dependence of R , which is our primary concern, is implicit in Eqs. (1) through (6) written below in the cgs system. R is given in terms of the index of refraction n and the extinction coefficient κ by

$$R = [(n-1)^2 + \kappa^2] / [(n+1)^2 + \kappa^2], \quad (1)$$

and n and κ are related to ϵ_1 and ϵ_2 by the defining equations

$$\epsilon_1 = n^2 - \kappa^2,$$

$$\epsilon_2 = 2n\kappa. \quad (2)$$

The dispersion relations derived from classical considerations of free-carrier effects are¹⁶

$$\epsilon_1 = \epsilon_\infty \sum_i \left[1 - \frac{\omega_{p,i}^2}{\omega^2 + \gamma_i^2} \right], \quad (3)$$

$$\epsilon_2 = \epsilon_\infty \sum_i \frac{\gamma_i \left(\frac{\omega_{p,i}^2}{\omega^2 + \gamma_i^2} \right)}, \quad (4)$$

where ϵ_∞ is the optical dielectric constant arising from the combined effects of bound charges, γ_i is a phenomenological damping constant, and $\omega_{p,i}$ is the plasma fre-

¹⁰ W. G. Spitzer and H. Y. Fan, *Phys. Rev.* **106**, 882. (1957).

¹¹ W. W. Duerig and I. L. Mador, *Rev. Sci. Instr.* **23**, 421 (1952).

¹² B. B. Houston, Jr., *Bull. Am. Phys. Soc.* **5**, 166 (1960).

¹³ R. F. Brebrick and E. Gubner, *J. Chem. Phys.* **36**, 1283 (1962); W. W. Scanlon, *Phys. Rev.* **126**, 509 (1962).

¹⁴ M. K. Norr, *J. Electrochem. Soc.* **109**, 433 (1962).

¹⁵ R. S. Allgaier and B. B. Houston, Jr., *Proceedings of the International Conference on the Physics of Semiconductors, Exeter* (The Institute of Physics and the Physical Society, London, 1962), p. 172.

¹⁶ Frank Stern, *Solid State Phys.* **15**, 299 (1963).

quency. The summation index i refers to the different types of free carriers contributing to ϵ_1 and ϵ_2 . γ_i and $\omega_{p,i}$ are related to the properties of the free carriers of type i by

$$\omega_{p,i} = [4\pi N_i e^2 / m_{s,i} \epsilon_\infty]^{1/2}, \quad (5)$$

$$\gamma_i = 1/\tau_i = e/m_{s,i} \mu_i, \quad (6)$$

where N_i is the carrier density, e is the magnitude of the electronic charge, $m_{s,i}$ is the electric susceptibility effective mass of the carriers, τ_i is the energy-independent scattering time, and μ_i is the carrier mobility. For the range of frequencies such that $\omega^2 \gg \gamma_i^2$ and $\kappa^2 \ll n^2$, the equations above can be simplified to give

$$R = (n-1)^2 / (n+1)^2, \quad (7)$$

$$\epsilon_1 = n^2 = \epsilon_\infty - (4\pi e^2 / \omega^2) (N_T / m_s), \quad (8)$$

where

$$N_T = \sum_i N_i,$$

$$1/m_s = \sum_i (f_i / m_{s,i}),$$

f_i is the fraction of carriers of type i . When only a single type of carrier is involved, these equations reduce to those given by Spitzer and Fan.¹⁰ Using Eqs. (7) and (8), values of m_s and ϵ_∞ can be extracted from the experimentally determined frequency dependence of R . A point of particular significance in this connection is that the analysis does not require knowledge of the carrier scattering mechanism.

B. Relationship of Susceptibility Mass to Energy Bands

The electric susceptibility mass m_s is defined by the relation

$$\chi_c = -N e^2 / \omega^2 m_s, \quad (9)$$

where χ_c is the free-carrier susceptibility and N is the total carrier concentration. Expressions for m_s in terms of energy-band parameters can be derived by evaluating the corresponding χ_c and applying Eq. (9). This procedure has been carried out for various simple band structures by Spitzer and Fan.¹⁰ They find for parabolic, spherical energy surfaces of effective mass m^* that

$$m_s = m^*, \quad (10)$$

and for parabolic ellipsoids of revolution having transverse and longitudinal mass parameters m_T and m_L that

$$\frac{1}{m_s} = \frac{1}{3} \left(\frac{2}{m_T} + \frac{1}{m_L} \right). \quad (11)$$

A type of energy surface which is of particular interest here is a nonparabolic, $\langle 111 \rangle$ prolate surface of revolution which results when only two components of the effective-mass tensor are determined by a small energy gap. This situation has been treated by Cohen in his study of the energy surfaces of bismuth.¹⁷ His Eq. (26)

describing the constant-energy surface can be rearranged to give¹⁸

$$E = \frac{\hbar^2}{2} \left\{ \frac{k_T^2}{m_T [1 + (1/E_g)(E + (\hbar^2 k_L^2 / 2m_L'))]} + \frac{k_L^2}{m_L} \right\}, \quad (12)$$

where k_T and k_L are the transverse and longitudinal wave numbers; m_T and m_L , the transverse and longitudinal band-edge masses; m_L' , the longitudinal mass of the interacting band; and E_g , the interaction gap. We shall refer to such surfaces as the Cohen model. However, in so doing, we do not wish to imply that Cohen has proposed the model for the case of PbTe. The appropriateness of this model for the valence band of PbTe is suggested by the results of Shubnikov-de Haas oscillatory-magnetoresistance measurements.^{2,3} The susceptibility mass associated with such surfaces can be evaluated as indicated in the Appendix. The result is

$$\frac{N_1}{m_s} = - \int_0^\infty \frac{\partial f_0}{\partial E} \mathfrak{N}_p(E) I(E_r) dE, \quad (13)$$

where E is the energy; $E_r = E/E_g$; f_0 is the Fermi-Dirac distribution function; N_1 , the concentration of carriers in one valley; $\mathfrak{N}_p(E)$, the number of states within a parabolic ellipsoid of energy E having mass parameters m_T and m_L . The term $I(E_r)$ is related to the band parameters by the following group of equations:

$$I(E_r) = \frac{I_T(E_r)}{m_T} + \frac{I_L(E_r)}{m_L}, \quad (14)$$

$$I_T(E_r) = \left(\frac{1+E_r}{1+2E_r} \right) \beta - \frac{[1-(b-1)E_r]}{(b-1)E_r} (1-\beta) - \frac{b}{(b-1)} \left[\frac{1}{3} - \frac{(1-\beta)}{\delta^2} \right], \quad (15)$$

$$I_L(E_r) = \frac{[1-(b-1)E_r]^2}{(b-1)E_r} (1-\beta) + \frac{4[1-(b-1)E_r]}{(b-1)} b \left[\frac{1}{3} - \frac{(1-\beta)}{\delta^2} \right] + \frac{4b^2}{(b-1)} E_r \left\{ \frac{1}{5} - \frac{1}{\delta^2} \left[\frac{1}{3} - \frac{(1-\beta)}{\delta^2} \right] \right\}, \quad (16)$$

in which

$$b = m_L / m_L',$$

$$\delta = [(b-1)E_r / (1+2E_r)]^{1/2},$$

$$\beta = \tan^{-1} \delta / \delta, \text{ when } m_L > m_L'$$

$$= \tanh^{-1} \delta / \delta, \text{ when } m_L < m_L'.$$

¹⁸ The term involving m_L' in Eq. (12) produces a deviation from an ellipsoidal relation. However, for the parameters which have been proposed the deviation is small. For this reason, such surfaces are sometimes referred to as being ellipsoidal.

¹⁷ M. H. Cohen, Phys. Rev. 121, 387 (1961).

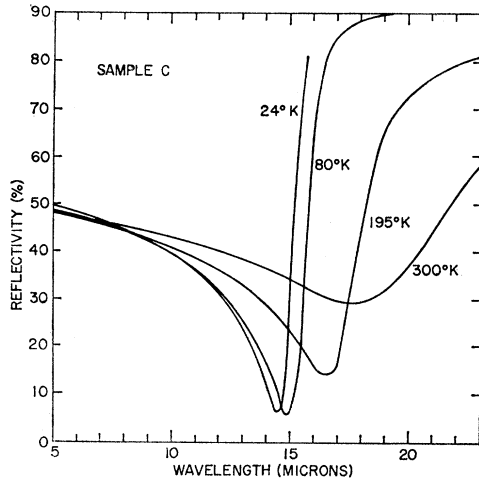


FIG. 2. Wavelength dependence of the normal reflectivity at various temperatures for *p*-type PbTe having a carrier concentration of $1.5 \times 10^{19} \text{ cm}^{-3}$. Experimental points have been omitted for graphical clarity. The density and scatter of the data are similar to those shown in Fig. 1.

The situation for which $m_L = m_L' (b=1)$ is applied in the analysis of our experimental data. In this case, the relations

$$I_T(E_r) = \frac{2}{(1+2E_r)} \left(\frac{1}{3} + \frac{2}{5} E_r \right), \quad (17)$$

$$I_L(E_r) = \frac{1}{(1+2E_r)} \left[\frac{1}{3} + \frac{4}{5} E_r + \left(\frac{4}{7} \right) E_r^2 \right], \quad (18)$$

are used along with Eqs. (13) and (14) to obtain m_s .

When $T=0$, Eq. (13) simplifies to

$$N_1/m_s = \mathfrak{N}_P(E_F) I(E_F/E_g), \quad (19)$$

where E_F is the Fermi energy. At this temperature, the concentration of carriers in one valley N_1 is equal to the number of states within a Cohen surface of energy E_F . It is shown in the Appendix that the number of states, $\mathfrak{N}_C(E)$, within a Cohen surface of energy E is given by

$$\mathfrak{N}_C(E) = \mathfrak{N}_P(E) \left[1 + E_r \left(1 + \frac{1}{5} b \right) \right]. \quad (20)$$

When these considerations are applied to Eq. (19), it becomes

$$\frac{1}{m_s} = \frac{I(E_F/E_g)}{1 + (E_F/E_g) \left(1 + \frac{1}{5} b \right)}. \quad (21)$$

The term $I(E_F/E_g)$ in this expression is evaluated using the appropriate relations given in the preceding paragraph.

IV. RESULTS

A. Reflectivity Data

Typical results of reflectivity measurements at near-normal incidence on *p*-type PbTe of various carrier concentrations and at various temperatures are shown in Figs. 1 and 2. The reflectivity curves have common

characteristics. At short wavelengths, the reflectivities approach a value of approximately 50%. This results from the contribution of bound electrons to the index of refraction, a contribution which is expected to be nearly independent of temperature and free-carrier concentration as indicated by the data. In the intermediate wavelength range, the reflectivity decreases to a minimum, a variation which results from the contribution of free carriers to the index. At longer wavelengths, the reflectivity becomes uniformly high, typical of metallic reflection.

B. Analysis

When the minimum reflectivity is small, as for the curves of Fig. 1, Eqs. (7) and (8) can be applied at frequencies between the reflectivity minimum and the fundamental absorption edge. Values of m_s and ϵ_∞ have been extracted from the reflectivity data by plotting the corresponding ϵ_1 's as illustrated in Fig. 3. Equation (8) shows that the slope of such a curve yields m_s and the intercept gives ϵ_∞ directly. Values of m_s obtained in this manner are plotted in Fig. 4 for various carrier concentrations and temperatures. These results are uncertain to $\pm 10\%$, and they include corrections which are discussed below.

The average value of ϵ_∞ for all temperatures and carrier concentrations was 32.6. This is in reasonable agreement with the value of 31.8 ± 0.3 reported by Walton and Moss¹⁹ on the basis of prism measurements. Our results indicate that ϵ_∞ decreases with increasing temperature and carrier concentration. However, since the variations involved are only slightly greater than the uncertainty of ± 2 in each experimental value of ϵ_∞ , no quantitative statement regarding these dependences can be made on the basis of our results.

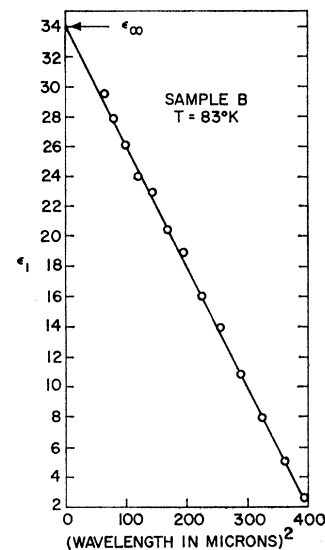


FIG. 3. Real part of the dielectric constant at 83°K for *p*-type PbTe having a carrier concentration of $5.7 \times 10^{18} \text{ cm}^{-3}$. The values were determined from the reflectivity data of Fig. 1 and Eqs. (7) and (8) given in the text.

¹⁹ A. K. Walton and T. S. Moss, Proc. Phys. Soc. (London) **B81**, 509 (1963).

C. Correction for Carrier Scattering

When the minimum reflectivity is not small, as in the curve for $T=300^\circ\text{K}$ of Fig. 2, the more general Eqs. (1) through (6) which take carrier scattering into account must be used to determine ϵ_∞ , m_s , and γ corresponding to the experimental reflectivity curves. This more complicated analysis was required for only a small number of our experimental points, those indicated in Fig. 4 by the filled-in symbols. These corrected values of m_s are smaller than those obtained from the simpler analysis described in Paragraph B. The maximum correction was 21%.

The method used to obtain these corrections was to find by trial calculations the values of ϵ_∞ , m_s , and γ which gave the best fit to an experimental reflectivity curve. The calculations were straightforward but numerous and were carried out on the 7090 IBM computer. In applying Eqs. (1) through (6), it was assumed that only one type of carrier was involved. There is evidence that this assumption is not realistic and that two types of carriers contribute to the electrical and optical properties, especially at temperatures above 150°K .^{4,7,9} The justification for our assumption is based upon the fact that good fits were obtained between calculated and experimental reflectivity curves. Nevertheless, because of the uncertainty regarding the types of carriers involved, the correction for carrier scattering which we have used should be considered first order in nature.

Typical values of the mobilities calculated from the scattering frequencies using Eq. (6) are listed in Table I as optical mobilities. It is interesting to compare these with the conductivity mobilities which were determined from measurements of the Hall coefficient and electrical conductivity. In all cases, the optical mobilities are smaller than the corresponding conductivity mobilities. It is possible that these differences are related to the fact that optical mobilities are characteristic of a relatively thin surface layer rather than the bulk of the material and that carrier scattering can be different in the two regions. The difference between the optical and conductivity mobilities of sample B is relatively small. This may be associated with the fact that this sample

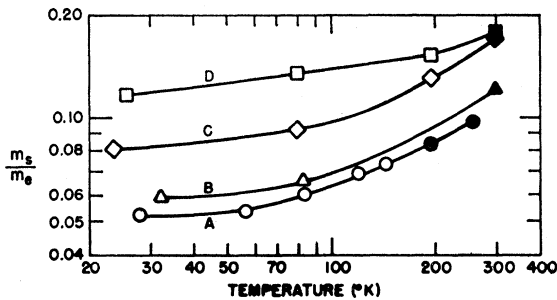


FIG. 4. Temperature dependence of electric-susceptibility mass for p -type PbTe samples having various carrier concentrations. Electrical properties of these samples are given in Table I. The filled-in symbols represent data which required correction for carrier scattering, as discussed in the text.

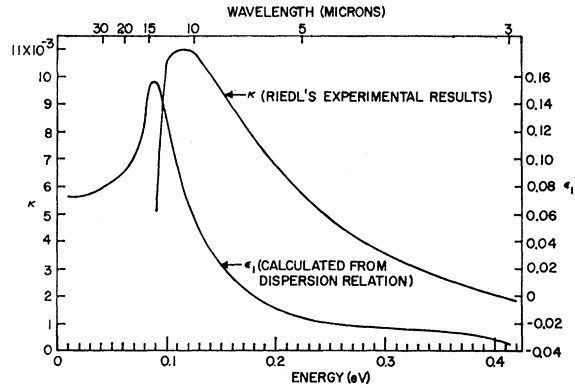


FIG. 5. Optical constants associated with the extra absorption in the free-carrier region of p -type PbTe. The constants apply to a sample at 300°K having a carrier concentration of $3.7 \times 10^{18} \text{ cm}^{-3}$. The real part of the dielectric constant ϵ_1 was calculated using a dispersion relation and Riedl's experimental extinction coefficients κ .

was the only one subjected to annealing (760°K for approximately one hour).

D. Correction for Lattice Dispersion

Lattice dispersion contributes a small but significant amount to the dielectric constant ϵ_1 measured in our experiments. This contribution produces an error in the value of m_s calculated as described above. Corrected values have been obtained using the relation¹⁶

$$\left(\frac{1}{m_s}\right)_{\text{corrected}} = \left(\frac{1}{m_s}\right) - 1.22 \times 10^{-48} \left(1 - \frac{\epsilon_\infty}{\epsilon_0}\right) \frac{\epsilon_\infty}{\lambda_L^2 N}, \quad (22)$$

where N is the carrier concentration, ϵ_0 is the static dielectric constant and λ_L is the wavelength in microns of the longitudinal optical mode. In applying Eq. (22), we have used the values of 400 for ϵ_0 reported by Kanai and Shohno,²⁰ and 91.2μ for λ_L as given by Hall and Racette.²¹ The resulting corrections increase the values of m_s from 1 to 15%.

E. Effect of Dispersion Due to Extra Absorption

An absorption which adds to the classical free-carrier effect at wavelengths just beyond the fundamental absorption edge has been observed and studied by Riedl.⁷ It is believed to arise from intravalence band transitions. The extinction coefficients κ associated with this extra absorption for a sample having a carrier concentration of $3.7 \times 10^{18} \text{ cm}^{-3}$ and a temperature of 300°K are shown in Fig. 5. These values have been used to calculate the corresponding ϵ_1 's. This has been done by applying the dispersion relation¹⁶

$$\epsilon_1(E) = -\frac{4}{\pi} \int_0^\infty \frac{E' n(E') \kappa(E')}{E'^2 - E^2} dE'. \quad (23)$$

²⁰ Y. Kanai and K. Shohno, Japan. J. Phys. 2, 6 (1963).

²¹ R. N. Hall and J. H. Racette, J. Appl. Phys. Suppl. 32, 2078 (1961).

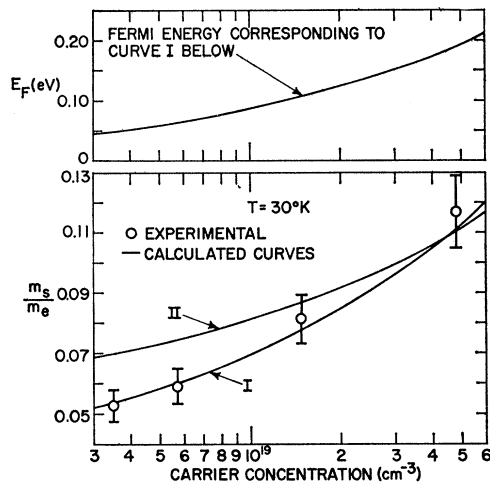


FIG. 6. Carrier-concentration dependence of the electric-susceptibility mass at 30°K. Curve I was calculated on the basis of the single-band Cohen model and the band-edge parameters given by Cuff *et al.* in Ref. 3. Curve II represents values of the susceptibility mass calculated for the two-band model described in the text. The upper curve gives the Fermi energies for holes corresponding to the Cohen model.

In performing the numerical integration, it has been assumed that the values of κ for energies beyond the range shown in the figure are zero. The indices of refraction n were determined experimentally from reflectivity measurements. The calculated results given in Fig. 5 are small in comparison with those associated with the usual free-carrier effect. The error in the determination of m_s caused by the extra absorption in such a sample is estimated to be less than 2%.

Riedl has shown that the intraband absorption decreases with temperature, and its significance to calculated values of m_s is expected to vary in the same way. In addition, it has been shown that the magnitude of this absorption is proportional to the carrier concentration in the range from 5.0×10^{17} to 3.7×10^{18} cm^{-3} . We have extrapolated this relationship in an effort to estimate the significance of this effect for our sample D. Calculations similar to those described above indicate that the extra absorption increases the experimental value of m_s by less than 4%. This is believed to be the largest possible error due to the extra absorption in our measurements since it applies to our highest carrier concentration and temperature. None of the data in Fig. 4 have been corrected for this small effect.

V. DISCUSSION

A. Carrier Concentration Dependence of m_s

The data of Fig. 4 show a strong dependence of m_s upon N , especially at low temperatures. This is illustrated more clearly in Fig. 6, where mass values applying to a temperature of approximately 30°K have been plotted. The large and continuous variation of m_s indicates that the energy bands involved are nonparabolic. This follows from the fact that the carrier-

concentration dependence of m_s arising from parabolic bands would be either independent of N or characterized by sharp breaks. The breaks would be associated with the carrier concentrations at which the Fermi level first enters another band of different mass. The nonparabolic behavior suggested by our data is consistent with the results reported by Cuff *et al.*,^{2,3} which show that the transverse mass associated with the $\langle 111 \rangle$ surfaces is strongly dependent upon N . They have interpreted this behavior in terms of the Cohen model described in Sec. III. B.

We have calculated the carrier concentration dependence of m_s , which would be expected at 30°K on the basis of the single-band, Cohen model. This was done by applying Eqs. (13) through (21). The results are plotted as Curve I in Fig. 6. The corresponding Fermi energies are given in the upper part of the figure. The calculations were based upon the parameters

$$\begin{aligned} m_T &= 0.022 m_e, \\ m_L &= 0.3 m_e, \\ E_g &= 0.14 \text{ eV}, \\ m_{L'} &= 0.3 m_e. \end{aligned}$$

The first three of these parameters were deduced by Cuff *et al.*³ from oscillatory-magnetoresistance data obtained at temperatures around 4°K. We have assumed that they are valid at 30°K, the temperature applying to the data of Fig. 6. The reasonableness of this assumption is supported by the relative insensitivity of m_s to temperature in the low-temperature region, as shown in Fig. 4. This insensitivity would be expected to extend down to 4°K, suggesting a corresponding small variation of the band parameters. Additional support for this assumption is afforded by the small variation of the optical gap over this temperature region.²² Our assumption that $m_L = m_{L'}$ is based upon the similarity of the $\langle 111 \rangle$ surfaces of the conduction and valence bands.² The major part of the interaction producing nonparabolicity is expected to be between these surfaces. Nevertheless, our assumption should be considered somewhat arbitrary since all of the interacting bands have not been definitely identified. Fortunately, the calculated values of m_s are very insensitive to m_L and $m_{L'}$ over a reasonable range of their values. For example, a change in our value of either m_L or $m_{L'}$ to $0.15 m_e$ or to $0.60 m_e$ produces variations of less than 5% in m_s throughout the range of carrier concentrations shown in Fig. 6. The interaction gap E_g is somewhat smaller than the optical gap of 0.19 eV at 4.2°K.²² A possible explanation is that there are more than two interacting bands producing the nonparabolicity. Models with more than two interacting bands have been considered by Dimmock and Wright.²³

²² D. L. Mitchell, E. D. Palik, and J. N. Zemel, *Physics of Semiconductors, Proceedings of the 7th International Conference, Paris* (Dunod Cie., Paris, 1964), p. 325.

²³ J. O. Dimmock and G. B. Wright, *Phys. Rev.* **135**, A821 (1964).

They show that these may sometimes be approximated by a two-band model involving an effective-interaction gap smaller than the optical gap.

The good agreement between calculation and experiment serves as evidence that a Cohen-type band is primarily responsible for the observed carrier-concentration dependence of m_s at low temperatures. This point is of particular significance because of conflicting reports regarding the existence of a $\mathbf{k}=0$ heavy-mass band with an edge at nearly the same energy as that of the $\langle 111 \rangle$ bands.^{2,4-6,24} Such a band would contribute to the magnitude of m_s and its dependence upon carrier concentration. To illustrate this, we have calculated the susceptibility mass corresponding to the two-band situation as a function of N . The calculation was based upon the relation

$$\frac{1}{m_s} = \frac{f_{SB}}{m_{SB}} + \frac{f_{CB}}{m_{CB}}, \quad (24)$$

in which f_{SB} and f_{CB} are fractions of the total carriers in the spherical and Cohen bands, respectively, and m_{SB} and m_{CB} are the corresponding susceptibility masses. The susceptibility mass of the Cohen band was calculated using the method and the band parameters described previously. The mass for the spherical band was determined using Eq. (10) and the effective mass of $0.15 m_e$ reported by Stiles, Burstein, and Langenberg.⁵ We have assumed that this band is parabolic and that its edge is at the same energy as the Cohen band.

Results of the calculations are plotted in Fig. 6. They show that both the magnitude and carrier-concentration dependence of m_s for this two-band case differ significantly from the observed behavior. We conclude that the existence of the heavy-mass band described above is not consistent with our experimental data. Allgaier has also concluded that there is no evidence from Hall data that a second band is occupied at low temperatures.⁴ Other Hall measurements and analysis support this conclusion up to a carrier concentration of $1 \times 10^{20} \text{ cm}^{-3}$.⁹

B. Temperature Dependence of m_s

The data of Fig. 4 also show that there is a pronounced temperature dependence of m_s for each of the samples. The behavior can be partially explained in terms of the single-band Cohen model. To demonstrate this, we have calculated the temperature dependence of m_s which would be expected on the basis of this model for samples A and D. The calculations were based upon the band parameters given above and the assumption that E_g varies linearly with temperature from 30°K. In addition, it was assumed that m_T and E_g are related by $m_T^{-1} = -1 + E_P'/E_g$. E_P' is the parameter given by Cuff *et al.* as 6.4 eV.³ It is related to an effective transverse momentum matrix element. Because of the in-

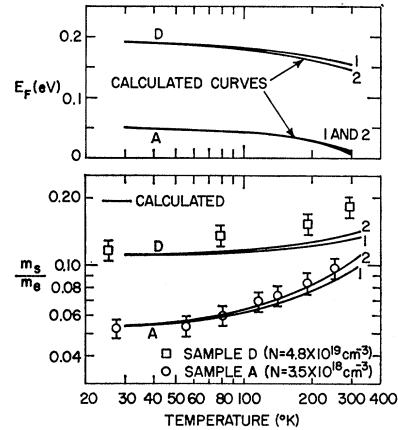


FIG. 7. Temperature dependence of the electric-susceptibility mass for p -type PbTe having carrier concentrations of 3.5×10^{18} and $4.8 \times 10^{19} \text{ cm}^{-3}$. The calculated curves were based upon the single-band Cohen model and an interaction gap which varies linearly with temperature. Curves 1 and 2 represent the results obtained for temperature coefficients of 4.9×10^{-4} and $6.7 \times 10^{-4} \text{ eV}/^\circ\text{K}$, respectively. The significance of these coefficients is discussed in the text. The upper curves give the corresponding values of the Fermi energy for holes.

sensitivity of m_s to both m_L and m_L' , we have taken them to be temperature-independent.

The results of our calculations are given in Fig. 7. These depend upon the value of the temperature coefficient α describing the linear temperature variation of E_g . The exact value of this coefficient is not known. For this reason, our calculations are based upon two approximations of α , represented by the two pairs of Curves 1 and 2. For Curves 1, we have used the value of α applying to the optical energy gap, E_{opt} . This value of $4.9 \times 10^{-4} \text{ eV}/^\circ\text{K}$ was determined from the experimental results of Scanlon at 300°K²⁵ and those of Mitchell *et al.* at low temperatures.²² The reasonableness of this assumption is based upon the belief that the major part of the interaction producing nonparabolicity is between the $\langle 111 \rangle$ surfaces in the conduction and valence bands. Therefore, E_g would be expected to vary with temperature in approximately the same way as E_{opt} , since the latter is a measure of the separation between extrema of these surfaces. For Curves 2, we have chosen an α of $6.7 \times 10^{-4} \text{ eV}/^\circ\text{K}$, so that at 300°K E_g is equal to E_{opt} or 0.32 eV. This value of α probably represents an upper limit, since E_g is not expected to become larger than E_{opt} . For the lower carrier concentration (sample A), there is agreement between calculation and experiment; both Curves 1 and 2 are within the limits of error of our experimental results. Thus the large temperature dependence of m_s for this sample can be adequately described in terms of the single-band Cohen model and a temperature-dependent interaction gap.

For sample D, the calculated curves are in agreement with experiment at 30°K, but they deviate from the

²⁴ Riro Nii, J. Phys. Soc. Japan **19**, 58 (1964).

²⁵ W. W. Scanlon, J. Phys. Chem. Solids **8**, 423 (1959).

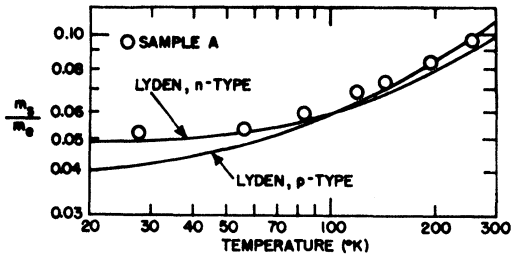


FIG. 8. Comparison of our results for the temperature dependence of the electric-susceptibility mass with those reported by Lyden in Ref. 26. The carrier concentration of our sample was $3.5 \times 10^{18} \text{ cm}^{-3}$. Lyden's results apply to several samples having carrier concentrations ranging from 2.2×10^{18} to $3.8 \times 10^{18} \text{ cm}^{-3}$.

data as the temperature is increased. The deviation may be related to the existence of a second band at lower energies. There is experimental evidence in the temperature range from 150 to 300°K that a second band exists with an edge approximately 0.1 eV below the extrema of the $\langle 111 \rangle$ surfaces.^{4,7,9} The Fermi energies E_F given in Fig. 7 for sample D indicate that m_s would be influenced by such a band in this temperature region. Conversely, the relatively small values of E_F associated with sample A suggest that the second band would contribute only a small amount to m_s at the lower carrier concentration. The mass of a single-valley second band required to bring Curves 1 and 2 into agreement with experiment for sample D at room temperature is $0.6 m_0$. This value was obtained from a two-band analysis similar to that described in Sec. V. A. This analysis was based upon a band separation of 0.08 eV estimated from the low-energy threshold of the extra absorption data of Riedl shown in Fig. 5. This extra absorption has been attributed to transitions from a second band to the $\langle 111 \rangle$ band, and the threshold is a measure of their separation. The good agreement between the single-band calculation and experiment at 30°K indicates that the second band is not occupied. By considering the corresponding Fermi energy, it can be concluded that at this temperature the second band is at least 0.19 eV below the Cohen band. Thus, it appears that the separation between the two bands increases as the temperature is lowered. Such a variation is consistent with the fact that the low-energy threshold of the extra absorption moves to higher energies as the temperature decreases.⁷

Despite the success of the single-band Cohen model for sample A, we cannot rule out the possibility that a second band is populated also, at least to a small extent. The uncertainties in our experimental values of m_s and the assumed temperature coefficients of E_g limit the significance of the agreement which we have obtained using the Cohen model. However, by taking all of these factors into consideration, we estimate that less than 20% of the carriers are in a second band at room temperature. We emphasize these points here because of the rather strong evidence based upon the

electrical measurements of Allgaier⁴ that a second valence band is occupied at this carrier concentration for temperatures above 150°K. Allgaier and Houston have extended these measurements, and their analysis leads to the prediction that about 10% of the carriers occupy the second valence band at 300°K.⁹ Recent work of Lyden²⁶ also supports this two-valence band model. He has measured m_s and the density-of-states mass m_d as a function of temperature for both p - and n -type PbTe. Carrier concentrations of his samples were approximately equal to that of our sample A. His results for m_s are presented in Fig. 8 and are in approximate agreement with ours.²⁷ Lyden's analysis of his results for n -type PbTe indicates that conduction band ellipsoids are responsible for the observed temperature dependence of m_s and m_d . From the p -type results, however, he concludes that, in addition to the valence band ellipsoids, a second band is occupied.

C. Significance of Calculations and Data

The values of m_s calculated on the basis of the Cohen model are sensitive to each of the parameters m_T and E_g but very insensitive to m_L and m_L' . Thus the good agreement between calculation and experiment at low temperatures described in Sec. V. A can be considered substantiation for both the Cohen model and the values of m_T and E_g reported by Cuff *et al.*³ It should be emphasized, however, that the agreement does not serve as an independent determination of these parameters. This arises from the fact that the good fit to our experimental data is not unique to these particular values of m_T and E_g ; other combinations of these quantities can be found which give equally good agreement.

A knowledge of the large variations of m_s as a function of carrier concentration and temperature is of particular significance because of its pertinence to investigations of the carrier-scattering mechanisms in PbTe. Such studies are often based upon measurements of the electrical conductivity as a function of these variables. The analysis of such data to obtain information about scattering mechanisms requires that the conductivity mass of the carriers m_c be known as a function of carrier concentration and temperature. Since m_c is identical to m_s , our results provide the required information.

VI. SUMMARY

We have observed large changes in the electric susceptibility hole mass of PbTe as the carrier concentration and temperature are varied. The carrier-concentration dependence at our lowest temperature, and the temperature dependence for our smallest carrier concentration can be explained on the basis of a single-band, Cohen-type nonparabolic model of $\langle 111 \rangle$ prolate

²⁶ H. A. Lyden, Phys. Rev. 135, A514 (1964).

²⁷ In Ref. 26, Lyden compares his data with our early results given in Ref. 8. These early results differ somewhat from our present ones because they were not corrected as described in Sec. IV.

surfaces of revolution. The band parameters used are those reported by Cuff *et al.* There is no evidence at low temperatures for the previously reported heavy mass band at $\mathbf{k}=0$ with an extremum near those of the ellipsoids. At our largest carrier concentration, the Cohen model fails to give the observed values of m_s as a function of temperature, except at our lowest temperatures near 30°K. This is possibly due to a second band which becomes populated at higher temperatures. Such a band has been suggested by the experimental work of others. We estimate from our results and the intraband absorption data of Riedl that at room temperature this second valence band has a mass of $0.6 m_e$ and is 0.08 eV below the ellipsoids. In making this estimate of mass, it is assumed that the second band consists of a single valley. The low-temperature interaction gap of the Cohen model is somewhat smaller than the corresponding optical gap. A possible explanation is that the interaction producing nonparabolicity involves more than two bands.

ACKNOWLEDGMENTS

We are grateful for several helpful discussions with Dr. R. S. Allgaier and Dr. J. R. Burke of our laboratory, Dr. John O. Dimmock and Dr. George B. Wright of the MIT Lincoln Laboratory, and Dr. Frank Stern of the IBM Watson Research Center.

Dr. Allgaier and Dr. Burke have applied the Cohen model in their studies of piezoresistance, Hall effect, and weak-field magnetoresistance in PbTe. We have benefited considerably from a knowledge of their results prior to publication. We are indebted to these associates, also, for several of the Hall and conductivity measurements used to characterize our optical samples.

APPENDIX

The derivation of Eq. (13) for the electric-susceptibility mass of free carriers occupying a Cohen energy surface, described by Eq. (12), is based upon an evaluation of the corresponding electric susceptibility χ_c . It follows directly from the relations given by Spitzer and Fan¹⁰ or Cardona *et al.*²⁸ that when the frequency of the excitation ω and the carrier-scattering time τ are such that $(\omega\tau)^2 \gg 1$, the electric susceptibility for a cubic crystal is given by

$$\chi_c = \frac{1}{3} \frac{e^2}{\omega^2} \frac{2}{(2\pi)^3} \frac{\Gamma}{\hbar} \int_0^\infty \frac{\partial f_0}{\partial E} \left[\int_{S_k} v dS_k \right] dE, \quad (25)$$

where Γ is the number of equivalent valleys, $v = (1/\hbar) \times |\nabla_k E|$, and S_k is one of the equivalent constant energy surfaces in \mathbf{k} space. By applying Eq. (9) to this relation,

²⁸ M. Cardona, W. Paul, and H. Brooks, *Helv. Phys. Acta* **33**, 329 (1960). These authors have carried out an analysis similar to ours, and their work is a helpful reference.

it becomes

$$\frac{N_1}{m_s} = -\frac{1}{3} \frac{2}{(2\pi)^3} \frac{1}{\hbar} \int_0^\infty \frac{\partial f_0}{\partial E} \left[\int_{S_k} v dS_k \right] dE, \quad (26)$$

where $N_1 = N/\Gamma$ is the carrier concentration in one valley. The relation is simplified by substituting

$$dS_k = 2\pi [|\nabla_k E| / |(\nabla_k E)_T|] k_T dk_L,$$

giving

$$\frac{N_1}{m_s} = -\frac{1}{3} \frac{4}{(2\pi)^2} \int_0^\infty \frac{\partial f_0}{\partial E} \left[\int_0^{k_L(\max)} \frac{v^2 k_T}{|(\nabla_k E)_T|} dk_L \right] dE. \quad (27)$$

The evaluation of the integral over k_L requires an expression for E as a $f(k)$. This is obtained from an algebraic rearrangement of Eq. (12) and is

$$2E = - \left[E_g + \frac{\hbar^2 k_L^2}{2m_L} (b-1) \right] + \left\{ \left[E_g + \frac{\hbar^2 k_L^2}{2m_L} (b+1) \right]^2 + 4E_g \frac{\hbar^2 k_T^2}{2m_T} \right\}^{1/2}. \quad (28)$$

These last two relations lead to the result

$$\frac{N_1}{m_s} = - \int_0^\infty \frac{\partial f_0}{\partial E} \mathfrak{X}_P(E) I(E_r) dE, \quad (29)$$

where

$$I(E_r) = \frac{I_T(E_r)}{m_T} + \frac{I_L(E_r)}{m_L},$$

$$I_T(E_r) = \int_0^1 \frac{\{[E_r+1] - [1 - (b-1)E_r]E_L - bE_rE_L^2\}}{[(1+2E_r) + (b-1)E_rE_L]} \times d(E_L^{1/2}),$$

$$I_L(E_r) = \int_0^1 \frac{\{[1 - (b-1)E_r] + 2bE_rE_L\}^2 E_L}{[(1+2E_r) + (b-1)E_rE_L]} d(E_L^{1/2}).$$

In these relations,

$$E_r = E/E_g \quad \text{and} \quad E_L = \hbar^2 k_L^2 / 2m_L E.$$

The integrals can be evaluated using standard tables, and the results give Eqs. (15) and (16) when $b \neq 1$, and Eqs. (17) and (18) when $b = 1$.

Equation (20) which relates $\mathfrak{X}_C(E)$ and $\mathfrak{X}_P(E)$ is derived by carrying out the integration

$$\mathfrak{X}_C(E) = \frac{2}{(2\pi)^2} \int_0^{k_L(\max)} k_T^2 dk_L, \quad (30)$$

using an expression for k_T obtained from Eq. (12).